Polymer Journal

AWARD ACCOUNTS
SPSJ Wiley Award Accounts

Network Topology–Mechanical Properties Relationships of Model Elastomers

*By Kenji URAYAMA**

We review our recent studies on the mechanical properties of model elastomers with well-characterized network structures. Model elastomers were prepared by end-linking precursor poly(dimethylsiloxane) (PDMS) of known molecular weight with multifunctional crosslinkers. We then strictly assessed the modern entanglement models for rubber elasticity on the basis of the stress–strain data under general biaxial strains covering almost the entire range of accessible deformations for the model PDMS networks. We also demonstrated marked extensibility of more than 3000% for the deswollen networks prepared by removing the solvent from the end-linked gels prepared in the diluted state. The highly deswollen networks comprising the considerably compact conformation (supercoil) exhibited unusually weak strain dependence of stress. We also studied the viscoelastic properties of PDMS networks containing either unattached free chains or pendant chains. The former systems provided a model system to investigate the dynamics of the guest chains in invariant networks. The dynamics of the guest chains, as functions of their own sizes as well as the mesh sizes of host networks, were compared with the predictions of reptation theories. With the model networks with pendant chains, we elucidated the correlation between the damping properties and the amount of pendant chains. The elastomers with highly irregular structures exhibited high damping almost independent of both temperature and frequency.

KEY WORDS: Elastomers / Gels / Rubber Elasticity / Rheology / Reptation / Entanglements /

Crosslinked polymer networks composed of flexible strands exhibit many unique properties that stem from their three-dimensional network structures: they behave as soft solids because they do not flow macroscopically owing to the presence of crosslinks, but they still possess a liquid nature due to the weak constraints at the crosslinks, allowing the micro-Brownian motion of network strands. Rubber elasticity—reversible large deformability under small external forces—is one of the salient characteristics of polymer networks, and hence, they are often called "elastomers." Elastomers are widely employed in industry, and the fundamental aspects of their physical properties have been extensively investigated over the past half century.[1,2] The molecular understanding of their physical properties, however, still remains incomplete because their network structures are not well characterized:[3] the rubbery networks prepared by random-crosslinking of the precursor chains have inhomogeneous structures with a broad length distribution of the network strands; in addition, the characterization of the strand length distribution in elastomers is not possible by current analytical techniques. However, end-linking end-reactive precursor chains of known molecular weight using multifunctional crosslinkers affords a tailor-made model network with a well-characterized structure.[4–6] To the first-order approximation (which is accurate in the case of the complete reaction), the molecular mass of the network strands between neighboring crosslinks (M_c) is identical to that of the precursor chains, and the junction functionality (f_e) is the same as the functionality of the crosslinker (Figure 1). To consider the effect of the incomplete reaction on M_c and f_e, the degree of the end-linking reaction (p) is estimated from the amount of soluble species extracted after the reaction. Then, the corrected values of M_c and f_e are evaluated using p with the aid of a nonlinear polymerization theory.[7] We have investigated the physical properties of model end-linked networks with known topolog-

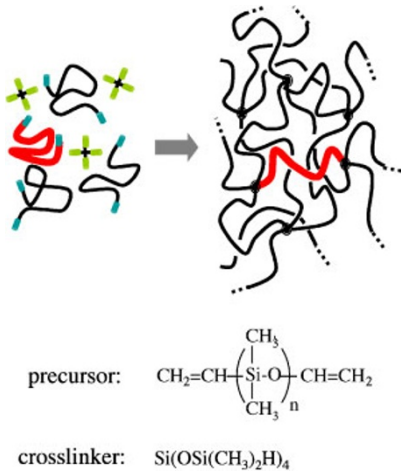

Figure 1. Schematic of the polymer network with well-characterized structure *via* end-linking of end-reactive precursors with tetrafunctional crosslinkers.

Department of Materials Chemistry, Kyoto University, Kyoto 615-8510, Japan
*To whom correspondence should be addressed (Tel: +81-75-383-2454, Fax: +81-75-383-2458, E-mail: urayama@rheogate.polym.kyoto-u.ac.jp).

ical characteristics to elucidate the topology–mechanical properties relationships of elastomeric networks. Vinyl-terminated poly(dimethylsiloxane) (PDMS) and tri- or tetrakisdimethylsiloxysilane were employed as the end-reactive precursor chains and the multifunctional crosslinker, respectively (Figure 1). The glass transition and crystal-melting temperatures of PDMS (*ca.* −120 and −40 °C, respectively) are far below room temperature.[8] The latter inhibits the stretching-induced crystallization. These thermal characteristics of PDMS merit the advantages for the fundamental studies on rubber elasticity.

The present paper reviews our studies on the multiaxial deformation behaviors of end-linked PDMS networks, the viscoelasticity of the networks containing unattached guest chains or a known amount of dangling chains, and the elongation properties of deswollen elastomers with marked extensibility.

MULTIAXIAL DEFORMATION BEHAVIORS OF END-LINKED PDMS NETWORKS

Molecular understanding of rubber elasticity is still far from the completion, although this area of study has a long history. One of the ultimate goals in the physics of rubber elasticity is the formulation of the elastic free energy (F_{el}) governing the stress–strain behaviors. If the form of F_{el} is known, we can determine, straightforwardly, the stresses (strains) under any type of deformation (stresses). Rubber elasticity has an entropic origin, and in principle, F_{el} can be theoretically derived by considering the manner in which the number of conformations available to the network strands changes under deformation. The main focus of modern molecular theories is on the modeling of the entanglement (uncrossability) effects of network strands, which is not considered in the classical theories.[2,9] The entanglements formed by different network strands act as additional crosslinks because they are not disentangled even in the long time limit owing to the presence of crosslinks; this is in contrast to the finite life times of transient entanglements in uncrosslinked polymer melts.[5,10–13] Many entanglement theories with different physical basis have been proposed, but most of the earlier attempts to experimentally verify these theories relied solely on the uniaxial deformation data. Several physically different models apparently predict the uniaxial data of the same elastomers.[14] This clearly indicates that we cannot evaluate the different molecular models solely on the basis of the uniaxial data. This is not surprising in view of the fact that uniaxial deformation is only one among all the accessible deformations. However, general biaxial strains varying independently along the two principal axes cover all the physically possible deformations for incompressible elastomers.[3,15] Nevertheless, there exist few experiments on the general biaxial deformations of elastomers, despite their importance.[16–18] The earlier biaxial experiments employed randomly crosslinked networks with obscure structural parameters. This also made the experimental assessment of the molecular theories ambiguous because the topological

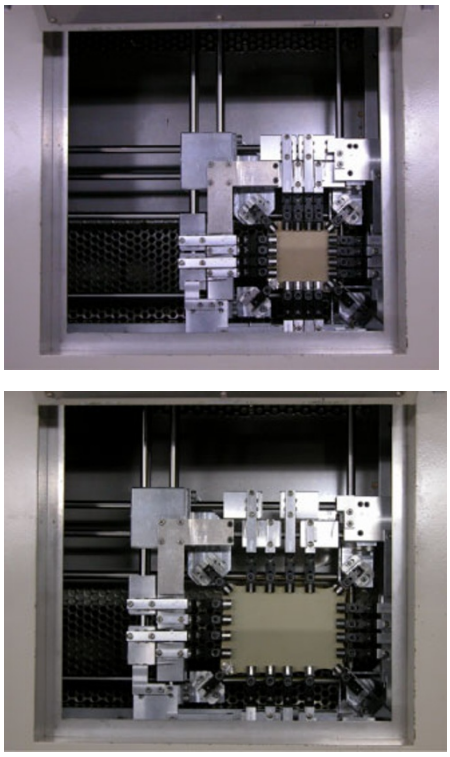

Figure 2. The biaxial tensile tester. (Upper) The undeformed state ($\lambda_1 = \lambda_2 = 1$). (Lower) The stretched state ($\lambda_1 = 2$ and $\lambda_2 = 1.5$). The sample is a sytrenebutadiene rubber.

parameters in the models were treated as adjustable parameters in the data-fitting stage.[19] On the other hand, the general biaxial deformations of elastomers with well-characterized structures can provide a basis to test, in an unambiguous fashion, these molecular entanglement models.

Figure 2 shows our custom-built biaxial tester (Iwamoto Seisakusho Co.).[20] The detectable minimum load is *ca.* 0.5 N and the maximum stretching strain is 400%. The specimen—a square sheet of *ca.* 4 cm width and 0.5 mm thickness—is clamped by four chucks on each of its four sides. The clamps are mounted on roller bearings so that they can move freely along the force detecting bars according to the applied deformation in the orthogonal direction. The tensile forces along the two directions are detected by two independent force-detection systems. Our instrument focuses on soft elastomers and gels with low moduli on the order of 10^4 Pa; this significantly differs from the earlier biaxial testers for conventional rubber vulcanizates with moduli on the order of 10^5 or 10^6 Pa.

Figure 3 illustrates the nominal biaxial stresses (σ_1 and σ_2) as functions of the principal ratios (λ_1 and λ_2) for an end-linked PDMS elastomer.[20] The inset shows the data of the uniaxial compression of the same sample. The weight-average molecular weight of the precursor PDMS ($M_w = 89{,}500$) is considerably higher than the critical molecular weight required to form entanglement couplings of PDMS (*ca.* 17,000). The precursor chains are highly entangled before end-linking, and the resultant network has many trapped entanglements. It

Polymer Journal

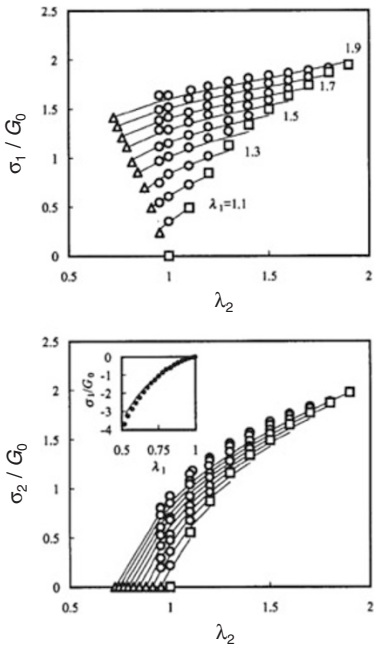

Figure 3. Equilibrium nominal biaxial stresses (σ_1 and σ_2) of an entanglement-dominated PDMS network as functions of the principal ratios. The network was prepared by end-linking long precursor PDMS with a volume fraction of 0.625 in the presence of inert oligomeric DMS (diluent). The stresses are reduced by the initial shear modulus G_0. The triangular and rectangular symbols represent uniaxial and equibiaxial stretching, respectively. The inset shows the data of uniaxial compression. The solid lines show the best-fitted results obtained by the slip-link model. Reproduced with permission from ref 27. Copyright (2001) American Chemical Society.

should be emphasized that the stresses in the figure correspond to the equilibrium values which exclude temporal effects: each set of biaxial stresses was measured at the corresponding strains after a small degree of stress relaxation was completed. Using this data, we assessed the five entanglement models—the diffused-constraint model,[21] the three different versions of the tube model,[22–24] and the slip-link model.[25,26] The elastic free energy of each model is composed of the two terms. The first term represents the contribution of the networks formed by chemical crosslinks. Most of the theories employ the form of the classical rubber elasticity theory or its modified form as the first term. The second term describes the entanglement effects, and the five models significantly differ in the second term. The diffused-constraint model considers that the trapped entanglements suppress the thermal fluctuation of chains but they do not additionally contribute to elastic modulus. In contrast, other four models argue that the entanglements act as additional cross-links and contribute to elastic modulus. The tube models consider each network strand is confined within a configurational tube with a harmonic potential. The three versions of the tube models employ different assumptions for the dependence of tube dimension on macroscopic deformation. The slip-link theory models the trapped entanglements as mobile slip-links, and it also considers the finite extensibility of network strands *via* the primitive path concept.

The molecular parameters such as the number of network strands and junctions included in the theories were not treated as free adjustable parameters in the data-fitting, but were compared with those evaluated using a nonlinear polymerization theory with the data of the soluble fractions independently of the mechanical testing results. The fitting results for each model were compared with those in the original reports.[27] As a result, we found that the quality of the data-fitting of four of the models (except the Edwards–Vilgis slip-link model) were not satisfactory. The solid lines in Figure 3 show the prediction of the slip-link model which most successfully accounts for the biaxial data. The full expression of F_{el} of the slip-link model is given by[25,26]

$$\frac{F_{el}}{RT} = \frac{1}{2}N_c\left[\frac{(1-\alpha^2)\sum\lambda_i^2}{1-\alpha^2\sum\lambda_i^2} + \ln\left(1-\alpha^2\sum\lambda_i^2\right)\right] + \frac{1}{2}N_s\left[\sum\left\{\frac{\lambda_i^2(1+\eta)(1-\alpha^2)}{(1+\eta\lambda_i^2)\left(1-\alpha^2\sum\lambda_i^2\right)} + \ln(1+\eta\lambda_i^2)\right\} + \ln\left(1-\alpha^2\sum\lambda_i^2\right)\right] \quad (1)$$

where Σ denotes the summation for i from 1 to 3, and N_c and N_s are the numbers of elastically effective network strands and slip-links, respectively. The model-specific parameters, η and α, characterize the slippage of the slip-link and the chain extensibility, respectively. These parameters are correlated with the topological characteristics of the networks *via* the relations $\eta \approx N_S/N_c$ and $\alpha^2 = N_j^{-1} = G_0 mp/(cRT)$, where N_j, G_0, m, p, and c are the number of the Kuhn segments between topologically adjacent junctions, the small-strain shear modulus, the molecular mass of a repeating unit, the number of the repeating units per Kuhn segment, and the network concentration, respectively.[26,28] The values for the sample in Figure 3 were evaluated to be $\eta = 0.130$ and $\alpha = 0.161$ from the structural parameters, independently of the data-fitting. These values are close to those ($\eta = 0.120$ and $\alpha = 0.160$) obtained by the best-fitting to the biaxial data. The agreements should be considered satisfactory in view of the accessible ranges of η and α ($0 < \eta < \infty$ and $0 < \alpha < 1$). The biaxial measurements were further performed for the three end-linked PDMS networks with different amounts of trapped entanglement.[29] The slip-link model was found to satisfactorily describe the biaxial data of these networks with the parameters of physically reasonable magnitudes.[30] After the publication of our report, some new entanglement theories[31,32] were proposed. Assessments using the biaxial data of model elastomers will be critical to prove the validity of these theories.

In addition to the validation of molecular theories, we estimated the phenomenological form of F_{el} as a function of the invariants of the deformation tensor that describes the biaxial data.[20,29] The estimated form is far more complicated than those of the classical theories as well as that of the familiar Mooney–Rivlin model. Thus, we pointed out, again, the lack of a physical basis for the Mooney–Rivlin plots, which have often

been employed for the analysis of the uniaxial data of elastomers,[20,33] although similar cautions have been raised in earlier works.[19,34,35]

ULTRA-HIGH EXTENSIBILITY OF DESWOLLEN PDMS NETWORKS

Reversible high extensibility is a salient characteristic of elastomers. This high extensibility results from the extension of network strands from the shrunken random-coiled state to the fully stretched state. The maximum elongation (λ_{max}) of a single polymer chain is given by the ratio of the end-to-end distances (R) between the two states: $\lambda_{max} = R_{max}/R_0 = (bN)/(bN^{1/2}) = N^{1/2}$, where b and N are the monomer length and the number of constitutive monomers, respectively.[36] This simply means that single polymer chains become more extensible as the contour length of the chains increases. We cannot, however, obtain highly extensible elastomers simply by end-liking long precursor chains. This is because the high overlapping of long precursor chains in the molten state results in the formation of trapped entanglements after end-linking. These trapped entanglements contribute to the rubber elasticity as additional crosslinks because they are not disentangled by stretching. For entanglement-dominated elastomers prepared by end-linking the long precursor chains comprising N monomers, $\lambda_{max,melt}$ is governed by not the number of monomers between adjacent chemical crosslinks (N) but that between neighboring entanglements ($N_{e,melt}$):

$$\lambda_{max} = {N_e}^{1/2} \tag{2}$$

The value of N_e is specific to each polymer, and the typical value is 20–40.[37] The resultant λ_{max} is around 5, which is not very far from the extensibility of conventional elastomers. As long as the crosslinking is performed in the molten state, λ_{max} is limited by eq 2 and is independent of the precursor length as well as the crosslinking density.

A simple way to reduce the trapped entanglements (*i.e.*, to increase N_e) is to perform the end-linking reaction in the diluted state with low overlapping degrees of the precursor chains. It is known that N_e is inversely proportional to the volume fraction ϕ of the precursor: $N_e = N_{e,melt}\phi^{-1}$.[37] The extensibility of the end-linked elastomers (gels) becomes larger than $\lambda_{max,melt}$ at $\phi = 1$ by a factor of $\phi^{-1/2}$. The solution-crosslinked elastomers contain a large amount of diluent (solvent). When the solvent in the gels is completely removed (*i.e.*, $\phi \to 1$), the networks exhibit macroscopic shrinkage (deswelling). If the affine deformation is assumed, R for the network strands decreases down to $R = R(\phi)\phi^{1/3}$ by full deswelling. Such deswollen networks originally prepared at low ϕ are expected to become markedly extensible:

$$\lambda_{max} = {N_{e,melt}}^{1/2}\phi^{-5/6} \tag{3}$$

Eq 3 shows that λ_{max} increases with decreasing ϕ, and that λ_{max} reaches 100 at the low ϕ (<0.03). The high extensibility of deswollen networks originates from two topological effects: a reduction in trapped entanglements, and a decrease in the end-to-end distance of network strands in the *unstretched* state. Both effects become larger with decreasing ϕ. The possibility of such highly extensible deswollen networks along this line was theoretically pointed out in ref 38.[38]

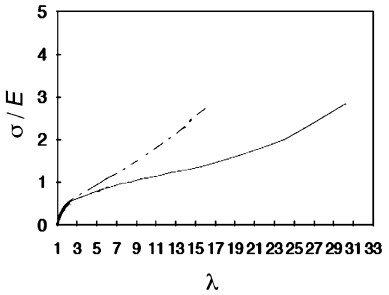

Figure 4. Nominal stress (σ)–elongation (λ) curves of the end-linked PDMS networks. The dash-dotted and solid lines represent the data of the networks prepared at $\phi = 0.1$ before and after deswelling, respectively, while the bold-solid line represents that the data of the network prepared at $\phi = 1$ (melt). The stress is reduced by the initial Young's modulus E of each sample. Reproduced with permission from ref 39. Copyright (1998) EDP Sciences.

We prepared deswollen networks by end-linking long precursor PDMS ($M_n = 99{,}000$) in the dilute state ($\phi = 0.1$). Figure 4 shows the nominal stress–elongation curves of the PDMS networks before and after deswelling.[39] Before deswelling, the network prepared at $\phi = 0.1$ is highly extensible up to $\lambda = 15$, while λ_{max} for that prepared in the molten state ($\phi = 1$) is around two. This indicates that the dilution at the crosslinking stage (*i.e.*, reduction in trapped entanglements) is effective in enhancing λ_{max}. The deswelling further increases λ_{max}, and in the fully deswollen state, λ_{max} reaches 31. This proves that the compact conformation of network strands formed by deswelling significantly contributes to the high extensibility. This high extensibility is entirely due to the entropic elasticity, and not because of plastic flow, since the deswollen networks exhibit perfect shape recovery even after the large stretching of $\lambda > 20$. The mechanical properties of the deswollen networks have been investigated by several researchers,[40,41] but none have reported such high extensibility. This is primarily because, in these earlier studies, ϕ was relatively high and the length of the precursor chains was not sufficiently long. The effect of ϕ on λ_{max} is systematically discussed in our paper.[42]

In addition to the high extensibility, unusually weak strain dependence of stress is also characteristic of the deswollen networks prepared at low ϕ. As can be seen in Figure 4, the gradient of the stress–elongation curve of the deswollen network is significantly smaller than that of the network before deswelling. The strain dependence of stress can be directly compared in the figure because the stress is normalized by the initial modulus of each sample. Figure 5 shows the double logarithmic plots of stress *vs.* $(\lambda - \lambda^{-2})$ for the highly extensible deswollen networks with $\phi = 0.1$ and 0.15. The term λ^{-2} stems from the lateral compression effect, but this becomes negligibly small in the large-λ region of interest. The λ dependence of stress is classified into the three regions: $\sigma \sim (\lambda - \lambda^{-2})$ in the region $1 < \lambda < 2$ (region I); $\sigma \sim (\lambda -$

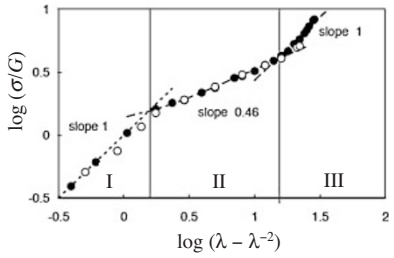

Figure 5. Double logarithmic plots of the reduced stress (σ/G) versus ($\lambda - \lambda^{-2}$) for the highly extensible deswollen networks prepared at $\phi = 0.1$ (closed symbols) and 0.15 (open symbols). Reproduced with permission from ref 39. Copyright (1998) EDP Sciences.

$\lambda^{-2})^{0.46} \approx \lambda^{0.46}$ in the region $2 < \lambda < 18$ (region II); and $\sigma \sim \lambda^{1.0}$ in the region $16 < \lambda < 31$ (region III). The behavior at small deformation (region I) agrees with the predictions of classical rubber elasticity theories. The behaviors at the large deformations of regions II and III were analyzed by the scaling law on the basis of the Pincus blob concept.[39] Pincus derived the λ dependence of σ for the high stretching of a single strand with fractal dimension D as[43,44]

$$\sigma \sim \lambda^{1/(D-1)} \tag{4}$$

Eq 4 is applicable to the highly stretched networks composed of the polymer chains of the fractal dimension D but without strong interactions between different network strands, because eq 4 is based on the single-chain approach. The highly deswollen networks are expected to satisfy this condition since they have few entanglements due to the low precursor concentration during synthesis. According to eq 4, the unusually weak dependence in region II originates from the compact conformation of the network strands in the deswollen state: eq 4 with $\sigma \sim \lambda^{0.46}$ results in $D = 3.2$, which is far larger than that ($D = 2$) for random-coiled chains. Region II corresponds to the pull-out process of the compact conformation. The dependence $\sigma \sim \lambda^{1.0}$ in region III leads to $D = 2.0$, which is identical to the fractal dimension of random-coils. The variation in the scaling exponent between regions II and III corresponds to the crossover in the responses from the unusually compact conformation to the usual Gaussian conformation.[38] The possibility of the formation of the compact conformation of network strands by deswelling was pointed out in early literatures,[44,45] wherein it was called *supercoil*. A small-angle neutron scattering study on the structure of labeled network strands revealed that the dimension in the deswollen state is considerably smaller than that in the unperturbed state.[46] We also observed the anomaly in the low-temperature crystallization behaviors of highly deswollen PDMS networks.[47] For moderately and lightly deswollen networks with $\phi > 0.2$, the degree of crystallization increases with decreasing ϕ as a result of the reduction in the number of trapped entanglements that act as defects for crystallization. In contrast, the highly deswollen networks with $\phi < 0.15$ exhibit smaller crystallization degrees. This result suggests that the compact conformation of the supercoil is disadvantageous for crystallization.

VISCOELASTICITY OF END-LINKED PDMS NETWORKS WITH UNATTACHED GUEST CHAINS

The dynamics of free guest chains trapped in polymer networks is a familiar classical issue in polymer physics.[44,48] This issue is also important as a basis to discuss the dynamics of polymer melts without crosslinks. In principle, the dynamics of the guest chains in crosslinked networks is a simpler problem than that in polymer melts, because the host matrix in the former is invariant due to crosslinks whereas that in the latter moves in a similar manner as the guest chains. The two important parameters that govern the motion of guest chains in crosslinked networks are their own size and the mesh size of the host networks (designated as M_g and M_x, respectively). De Gennes theoretically classified the types of guest-chain dynamics as functions of M_x and M_g,[49] and corresponding experiments were reported by several researchers.[50–52] But these earlier studies had some drawbacks: the mesh size was not precisely controllable owing to random crosslinking and/or the difference in chemical structure between the host networks and guest chains complicated the data interpretation. We prepared elastomeric networks with well-defined mesh sizes and containing guest chains with identical chemical structures by end-linking reactive PDMS in the presence of a small amount of inert linear PDMS. Two host networks with $M_x > M_e$ (NL) and $M_x < M_e$ (NS), where M_e is the molecular mass between neighboring entanglements in the melt ($M_e = 8{,}100$ for PDMS), were prepared by using long and short precursor chains of $M_n = 84{,}000$ and 4,550, respectively.

Figure 6 shows the angular frequency (ω) dependencies of the dynamic Young's modulus (E') and loss tangent ($\tan\delta$) for NL containing guest chains with various M_g.[53] The master curves in the figure were obtained by using the time–temperature superposition principle with data obtained at different temperatures. The E' and $\tan\delta$ curves for NS with guest chains were obtained by a similar method, although the data are not shown here. The values of M_x for NL and NS were evaluated to be $1.2M_e$ and $0.7M_e$ from the quasi-plateau modulus using the relation $E_{eq} = 3cRT/M_x$, where c is the network concentration. The $\tan\delta$ curves show a definite peak at a certain frequency, which shifts to the lower-ω region with increasing M_g. The maximum peak of the $\tan\delta$ curve is attributable to the viscoelastic relaxation of the guest chains, and the inverse of ω_{peak} corresponds to the characteristic time τ_g for the guest chains: $\tau_g = \omega_{peak}{}^{-1}$.

Figure 7 illustrates the M_g dependence of τ_g for NL and NS for a comparison with the theoretical predictions. The original reptation (tube) model[44,48,54] predicts a cubic power dependence of the longest relaxation time τ_L on M_g ($\tau_L \sim M_g{}^3$) in invariant (fixed) networks. The reptation model considering the correction for the contour length fluctuation (CLF) of the tube affords the expression for τ_L:[48,55]

$$\tau_L = \frac{b^2\zeta_0 M_g{}^3}{M_x M_0{}^2 \pi^2 kT}\left[1 - 1.3\left(\frac{M_x}{M_g}\right)^{0.5}\right]^2 \tag{5}$$

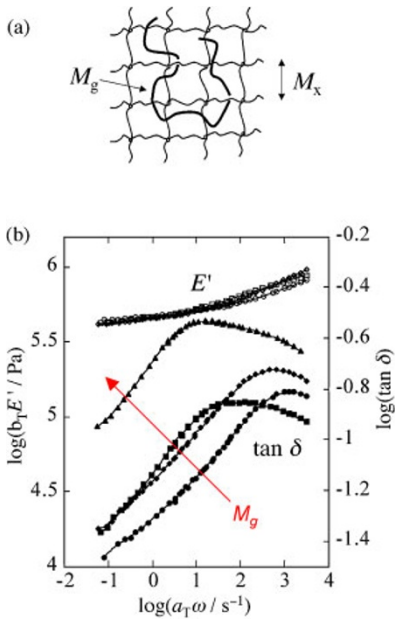

Figure 6. (a) Schematic of a guest linear chain trapped in a host network. (b) Master curves of angular frequency ω dependence of dynamic storage Young's modulus E' (open symbols), and the loss factor $\tan\delta$ (closed symbols) for the entanglement-dominated PDMS networks (NL) containing unattached linear PDMS. The reference temperature is 30 °C. The E' data for the pure networks without guest chains are represented by the crossed symbols, and the $\tan\delta$ data are outside the range of the figure due to their small magnitude. Weight-average molecular mass of the guest PDMS (M_g): circle, 1.14 × 10^5; diamond, 1.38 × 10^5; rectangle, 2.85 × 10^5; triangle, 3.54 × 10^5 g/mol. Reproduced with permission from ref 53. Copyright (2001) American Chemical Society.

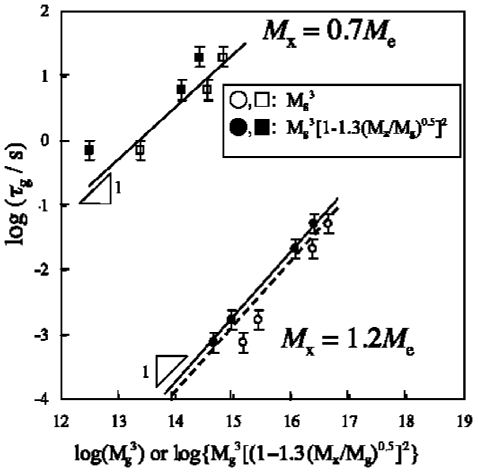

Figure 7. Dependence of the characteristic time (τ_g) on the weight-average molecular mass of guest linear chains (M_g) for the two end-linked PDMS networks with $M_x = 1.2M_e$ (circle) and $M_x = 0.7M_e$ (rectangular). The dashed straight line depicts the longest relaxation time τ_L predicted by the reptation theory with the CLF correction (eq 5) using the parameters of the PDMS melt. The slopes of the solid straight lines are equal to unity. Reproduced with permission from ref 53. Copyright (2001) American Chemical Society.

where b^2 is the mean-square end-to-end distance per monomer unit; ζ_0, the monomeric friction coefficient; and M_0, the monomeric molar mass. The expression in brackets corresponds to the correction term for the CLF. In principle, τ_g does not strictly coincide with τ_L but should be proportional to τ_L. Actually, as can be seen in Figure 6, τ_L calculated from eq 5 with the molecular parameters of PDMS melt is slightly smaller but close to τ_g for the entanglement-dominant network NL. The M_g dependence of τ_g for NL approximated by $\tau_g \sim M_g^{3.6}$ is appreciably stronger than the M_g^3 dependence of the original reptation model, but it is well described by the reptation model with the CLF correction. For the tightly crosslinked network NS, the M_g dependence of τ_g is closer to the cubic power law than the prediction with the CLF correction. The reptation model satisfactorily describes the M_g dependence of τ_g, independently of M_x.

For the same M_g, τ_g for NS is far larger than that for NL—by a factor of nearly 10^5. Although direct comparison is prevented by this remarkable difference, the difference in τ_g is straightforwardly estimated by extrapolation using the available data. On the basis of eq 5, De Gennes[49] predicted a *strangulation* effect, *i.e.*, a considerable slowing-down of reptation in tightly crosslinked networks with $M_x < M_e$ by a factor of M_x^{-1}. This prediction originates solely from the reduction in mesh size. Evidently, the dramatic slowing-down of reptation in NS cannot be explained by the strangulation effect, since the reduction factor of M_x is only *ca.* 2. According to eq 5, the remarkable slowing-down is apparently attributable to a marked increase in the segmental friction coefficient ζ_0 in NS. The temperature shift factors a_T at each temperature for constructing the master curves are the same for NL and NS. This suggests that there is no appreciable difference in free volume between the two networks, and the increase in ζ_0 is not attributable to an increase in T_g. The marked difference in ζ_0 may originate from the significant difference in the mesh characters of NS and NL. The mesh of NL is mainly formed by chain entanglements, while that of NS is primarily governed by chemical crosslinks. Moreover, a high crosslink density is expected to lower the mobility of network chains. Actually, a proton NMR study[56] on the dynamics of end-linked PDMS networks showed that the mobility of the network strands in networks prepared from precursors with $M_n < M_e$ is remarkably lower than that in the networks prepared from precursors with $M_n > M_e$, while the mobility is almost independent of M_n in the region $M_n > M_e$. The significantly lower mobility of the crosslink-dominant network matrix (NS) relative to the entanglement-dominant one (NL) may be one cause for the marked slowing-down of the dynamics of guest chains. It should be noted that the difference in mesh character between host networks with $M_x > M_e$ (entanglement-dominant) and $M_x < M_e$ (crosslink-dominant) is unavoidable in the experiments. This precludes exclusive observations of the influence of a tight mesh size without the effect of the mesh character in the regime $M_x < M_e$.

The dynamics of nonlinear polymers such as star-, comb-, and H-shaped polymers has been extensively investigated in their molten states without crosslinks.[57] Thus, the dynamics of such nonlinear polymers trapped in crosslinked networks is an interesting issue. Vega *et al.*[58] reported the viscoelastic

relaxation behaviors of model elastomers containing unattached star-shaped polymers, concluding that the guest star-shaped polymers and corresponding linear polymers pendant to host networks exhibit similar dynamics because of the immobility of the gravity center of the star-shaped polymers. However, there still appears to be much more to do before we arrive at a complete understanding of guest-chain dynamics.

DAMPING PROPERTIES OF END-LINKED PDMS NETWORKS WITH MANY PENDANT CHAINS

"Damping materials" used to suppress vibration and noise are of considerable demand in industry. For this purpose, the viscous effects of polymers, which dissipate vibration energy as heat, are employed as the damping mechanism.[59] The loss tangent ($\tan\delta$)—the ratio of the loss modulus (E'') to the storage modulus (E')—is often employed as a measure of the dissipation of deformation energy.[37] Usually, the viscoelasticity of polymers significantly depends on the time scale (frequency) as well as the temperature. A desirable damping material possesses a constant, high $\tan\delta$ over broad temperature and frequency ranges. To realize this property, many efforts have been made to blend polymers of low and high T_g,[60] or interpenetrate polymer networks with different T_gs,[61,62] since $\tan\delta$ becomes large at the glass transition. However, the approaches relying on the glass transition have some flaws: the optimized temperature regions are not sufficiently broadened, and a large change in E' at temperatures around T_g is unavoidable due to the drastic transition from the glassy state to the rubbery state. These characteristics limit the availability of materials for industrial use.

An ideal damping property, $\tan\delta \approx 1$ over a broad frequency range, is observed in a gelling material at the critical gel point—the intermediate state between the solid and liquid states.[63] This characteristic viscoelasticity of critical gels originates from their treelike fractal structure comprising many branched chains. However, critical gels are too soft for practical use as damping materials owing to the extremely low fraction of the elastic network backbone (the elastic part excluding any dangling chains from the network structure). The viscoelasticity of critical gels, however, provides some hints toward enhancing the damping properties of elastomeric materials. Two approaches are effective in obtaining temperature- and frequency-insensitive damping elastomers: one is to introduce a considerable amount of pendant chains into a developed infinite network, and the other is to use a moderately matured infinite network (still possessing high structural irregularity) slightly above the gelation threshold.

To demonstrate these concepts, we prepared such irregular elastomeric networks by end-linking linear PDMS chains with a trifunctional crosslinker. The end-linking method enabled us to create "model irregular networks" with known topological parameters such as the number of elastic chains, crosslinks, and pendant chains.[5,7,64] We then used them to elucidate the correlation between the amount of pendant chains and the viscoelastic properties of the networks.[64]

Two different schemes (Schemes A and B) were employed to prepare the irregular PDMS networks. In Scheme A, mixtures of bifunctional and monofunctional PDMS (with $M_n = 29{,}600$ and 25,700, respectively) were end-linked with the trifunctional crosslinker. The monofunctional precursor was incorporated into the network as a pendant chain, which is a major origin of the irregular structure. The molar ratio of silane–hydrogen in the crosslinker to the vinyl group in the precursors (r) was 1.3 for all the mixtures. In Scheme B, bifunctional precursors were end-linked with the trifunctional crosslinker at various off-stoichiometric ratios ($r \neq 1$): the reaction was conducted under imbalanced conditions in terms of the amounts of precursor and crosslinker. The end-linking at off-stoichiometric ratios led to an irregular network structure with structural defects such as dangling chains due to the presence of excess precursor or crosslinker.

Figure 8 shows the temperature dependence of E' and $\tan\delta$ for the irregular PDMS networks *via* Scheme B with various r at a frequency of 10 kHz. The data do not contain the contribution of unattached guest chains since the rheological measurements were conducted after the soluble materials not incorporated into the networks were extracted. The loss tangent is weakly dependent on temperature, and it increases with the deviation from the stoichiometric ratio ($r = 1$):$r = 0.70$ (the most excessive condition of precursor) leads to the largest $\tan\delta$ ($\approx$0.3), while $\tan\delta$ at $r = 1$ is the smallest among all the samples. No macroscopic gelation occurred at the conditions $r < 0.70$ and $r > 1.8$. A quantitative comparison between $\tan\delta$ and the amount of pendant parts (w_{pen}) is shown in Figure 9(b). The values of w_{pen} were evaluated from the fractions of soluble

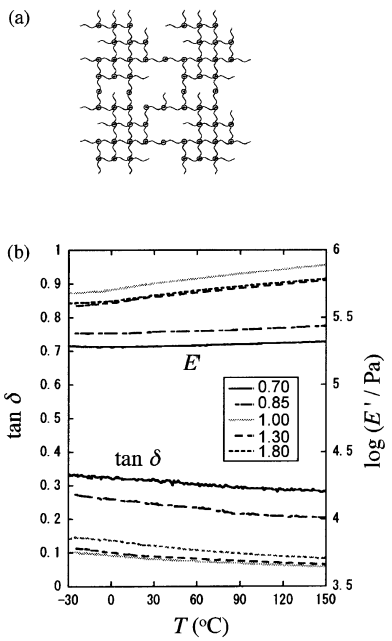

Figure 8. (a) Schematic of an irregular network with many pendant chains. (b) Temperature dependencies of the dynamic Young's modulus (E') and loss factor ($\tan\delta$) for irregular PDMS networks prepared at various r *via* Scheme B. Reproduced with permission from ref 64. Copyright (2004) American Chemical Society.

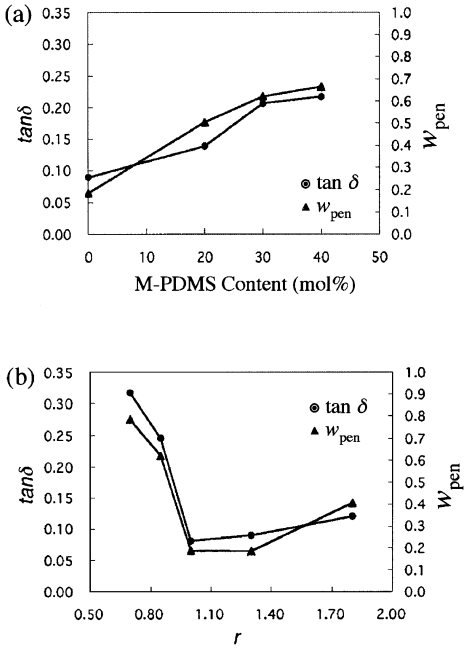

Figure 9. Loss factor (tan δ) and amount of pendant parts (w_{pen}) as a function of (a) the content of monofunctional PDMS in Scheme A and (b) r in Scheme B. Reproduced with permission from ref 64. Copyright (2004) American Chemical Society.

materials and the conditions of end-linking with the aid of the nonlinear polymerization model.[5,7,64] Evidently, tan δ and w_{pen} have a strong correlation, and tan δ increases with w_{pen}. The same trend was observed for the irregular networks obtained *via* Scheme A with various contents of monofunctional PDMS, as shown in Figure 9(a). It is found from Figure 9(a) and 9(b) that the networks with the same w_{pen} have similar tan δ, irrespective of the preparation route. This shows that the damping characteristic of elastomers is primarily governed by the amount of pendant parts. For the irregular network with the highest tan δ (≈ 0.3), w_{pen} is near 80% and the elastic part ($1 - w_{pen}$) is only *ca.* 20%. There is a tradeoff relation between the storage modulus and damping: The network with the highest damping has the lowest E' because it has the smallest amount of elastic chains.

In addition to the high tan δ, the insensitivity of tan δ and E' to temperature and frequency are also characteristic of the irregular networks. They are almost constant in the broad temperature range of $-30\,^{\circ}\mathrm{C} < T < 150\,^{\circ}\mathrm{C}$, although E' slightly increases with temperature due to the entropic elasticity. The markedly broad relaxation spectra stem from the irregular network structure comprising hierarchical branching parts of various sizes. It is known that a star-shaped polymer has a considerably broader relaxation spectrum than the corresponding linear polymer owing to a rich variety of relaxation modes.[37,57] The viscoelastic relaxation of the irregular networks is qualitatively similar to that of star- or branched polymers, but the quantitative interpretation is much more complicated because of the remarkably broad size distributions of the branched parts in the irregular structures. It should be noted that the damping mechanism relying on the viscoelastic relaxation of topologically irregular structures is universal for rubbery materials and is independent of the chemical structures of the rubbers. A considerable damping effect resulting from the pendant chains was also observed for a smectic liquid-crystal elastomer in the high-temperature isotropic state.[65] The temperature and frequency-insensitive high damping of irregular elastomeric networks provides a new approach for damping rubbers.

SUMMARY

We reviewed our recent studies on the mechanical properties of end-linked PDMS networks with well-characterized topological characteristics.

Several modern molecular entanglement models were strictly assessed on the basis of the stress–strain data under general biaxial deformation, covering almost the entire range of accessible deformations for incompressible elastomers. The molecular parameters used in the data-fitting were critically compared with those evaluated from the conditions of end-linking reactions, independently of mechanical testing data. The slip-link model was found to be the most successful in describing the biaxial data of networks with different amounts of trapped entanglement.

The deswollen networks prepared by removing the solvent from end-linked gels synthesized from dilute precursors exhibited marked extensibility of over 3000%. This remarkable extensibility stems from the small amount of trapped entanglement which acts as additional crosslinks, as well as the considerably compact conformation (supercoil) of the network strands with small end-to-end distances. The supercoil conformation results in unusually weak strain dependence of stress as well as the lowering of the low-temperature crystallizability.

The dynamics of free guest chains in end-linked networks was studied as a function of the mesh size and the length of the guest chains. The reptation model and its modified version well describe the manner in which the characteristic time of the guest chains varies with their chain lengths. The reptation of the unattached chains in tightly crosslinked networks whose mesh sizes are smaller than the entanglement spacing showed a marked slowing-down (by a factor of 10^5) as compared to that in the entanglement-dominated networks. This remarkable slowing-down in the tightly crosslinked networks cannot be explained by the existing models. The possibility of the effect of the difference in mobility of the host network matrices was pointed out.

The viscoelasticity of irregular PDMS networks with known amounts of pendant chains was examined. The damping of the networks increased with the amount of pendant parts, and irregular networks with a large fraction of pendant parts had remarkably broad relaxation spectra and high relaxation strength. The introduction of topological irregularity into network structures is a new approach to creating temperature- and frequency-insensitive high-damping elastomers.

Acknowledgment. The author thanks Prof. Emer. Kohjiya and Prof. Takigawa of Kyoto University for the helpful discussions. The author appreciates Dr. Takanobu Kawamura (Kanazawa Univ.), Messrs. Keisuke Yokoyama (NSK Ltd.), and Takashi Miki (Sumitomo Rubber Ind.) for their cooperation in the experiments. This work was partly supported by the Grant-in-Aid on Priority Area "Soft Matter Physics" (No. 19031014) and that for Scientific Research (B) (No. 16750186). This research was also supported in part by the Global COE Program "International Center for Integrated Research and Advanced Education in Materials Science" (No. B-09) of the Ministry of Education, Culture, Sports, Science and Technology (MEXT) of Japan, administrated by the Japan Society for the Promotion of Science.

Received: February 1, 2008
Accepted: March 27, 2008
Published: May 21, 2008

REFERENCES

1. L. R. G. Treloar, "The Physics of Rubber Elasticity," Clarendon Press, Oxford, 1975.
2. J. E. Mark and B. Erman, "Rubberlike Elasticity: A Molecular Primer," 2nd ed., Cambridge University Press, Cambridge, 2007.
3. K. Urayama, *J. Polym. Sci., Part B: Polym. Phys.*, **44**, 3440 (2006).
4. K. O. Meyers, M. L. Bye, and E. W. Merril, *Macromolecules*, **13**, 1045 (1980).
5. S. K. Patel, S. Molone, C. Cohen, J. R. Gillmor, and R. H. Colby, *Macromolecules*, **25**, 5241 (1992).
6. J. E. Mark, *Acc. Chem. Res.*, **37**, 946 (2004).
7. D. R. Miller and C. W. Macosko, *Macromolecules*, **9**, 206 (1976).
8. S. J. Clarson and J. A. Semlyen, "Siloxane Polymers," Prentice Hall, New Jersey, 1993.
9. M. Rubinstein and R. H. Colby, "Polymer Physics," Oxford University Press, Oxford, 2003.
10. N. R. Langley, *Macromolecules*, **1**, 348 (1968).
11. L. M. Dossin and W. W. Graessley, *Macromolecules*, **12**, 123 (1979).
12. K. Urayama and S. Kohjiya, *J. Chem. Phys.*, **104**, 3352 (1996).
13. K. Urayama, T. Kawamura, and S. Kohjiya, *J. Chem. Phys.*, **105**, 4833 (1996).
14. M. Gottlieb and R. J. Gaylord, *Polymer*, **24**, 1644 (1983).
15. N. W. Tschoegl and C. Gurer, *Macromolecules*, **18**, 680 (1985).
16. L. R. G. Treloar, *Trans. Faraday Soc.*, **40**, 0059 (1944).
17. J. Glucklich and R. F. Landel, *J. Polym. Sci., Part B: Polym. Phys.*, **15**, 2185 (1977).
18. S. Kawabata, M. Matsuda, K. Tei, and H. Kawai, *Macromolecules*, **14**, 154 (1981).
19. M. Gottlieb and R. J. Gaylord, *Macromolecules*, **20**, 130 (1987).
20. T. Kawamura, K. Urayama, and S. Kohjiya, *Macromolecules*, **34**, 8252 (2001).
21. A. Kloczkowski, J. E. Mark, and B. Erman, *Macromolecules*, **28**, 5089 (1995).
22. R. J. Gaylord and J. F. Douglas, *Polym. Bull.*, **23**, 529 (1990).
23. M. Kaliske and G. Heinrich, *Rubber Chem. Technol.*, **72**, 602 (1999).
24. M. Rubinstein and S. Panyukov, *Macromolecules*, **30**, 8036 (1997).
25. S. F. Edwards and T. A. Vilgis, *Polymer*, **27**, 483 (1986).
26. S. F. Edwards and T. A. Vilgis, *Rep. Prog. Phys.*, **51**, 243 (1988).
27. K. Urayama, T. Kawamura, and S. Kohjiya, *Macromolecules*, **34**, 8261 (2001).
28. T. A. Vilgis and B. Erman, *Macromolecules*, **26**, 6657 (1993).
29. T. Kawamura, K. Urayama, and S. Kohjiya, *J. Polym. Sci., Part B: Polym. Phys.*, **40**, 2780 (2002).
30. K. Urayama, T. Kawamura, and S. Kohjiya, *J. Chem. Phys.*, **118**, 5658 (2003).
31. M. Rubinstein and S. Panyukov, *Macromolecules*, **35**, 6670 (2002).
32. B. Mergell and R. Everaers, *Macromolecules*, **34**, 5675 (2001).
33. T. Kawamura, K. Urayama, and S. Kohjiya, *J. Soc. Rheol. Jpn.*, **31**, 213 (2003).
34. S. Kawabata and H. Kawai, *Adv. Polym. Sci.*, **24**, 89 (1977).
35. Y. Fukahori and W. Seki, *Polymer*, **33**, 502 (1992).
36. W. Kuhn, *J. Polym. Sci.*, **1**, 380 (1946).
37. J. D. Ferry, "Viscoelastic Properties of Polymers," 3rd ed., John Wiley & Sons, New York, 1980.
38. S. P. Obukhov, M. Rubinstein, and R. H. Colby, *Macromolecules*, **27**, 3191 (1994).
39. K. Urayama and S. Kohjiya, *Eur. Phys. J. B*, **2**, 75 (1998).
40. R. M. Johnson and J. E. Mark, *Macromolecules*, **5**, 41 (1972).
41. V. G. Vasiliev, L. Z. Rogovina, and G. L. Slonimsky, *Polymer*, **26**, 1667 (1985).
42. K. Urayama and S. Kohjiya, *Polymer*, **38**, 955 (1997).
43. P. Pincus, *Macromolecules*, **9**, 386 (1976).
44. P. G. de Gennes, "Scaling Concepts in Polymer Physics," Cornell University Press, New York, 1979.
45. W. W. Graessley, *Adv. Polym. Sci.*, **16**, 1 (1974).
46. C. Picot, *Prog. Colloid. Polym. Sci.*, **75**, 83 (1987).
47. K. Urayama, K. Yokoyama, and S. Kohjiya, *Polymer*, **41**, 3273 (2000).
48. M. Doi and S. F. Edwards, "The Theory of Polymer Dynamics," Oxford University Press, Oxford, 1986.
49. P. G. de Gennes, *Macromolecules*, **19**, 1245 (1986).
50. O. Kramer, R. Greco, R. A. Neira, and J. D. Ferry, *J. Polym. Sci., Part B: Polym. Phys.*, **12**, 2361 (1974).
51. K. Adachi, T. Nakamoto, and T. Kotaka, *Macromolecules*, **22**, 3111 (1989).
52. S. Ndoni, A. Vorup, and O. Kramer, *Macromolecules*, **31**, 3353 (1998).
53. K. Urayama, R. Yokoyama, and S. Kohjiya, *Macromolecules*, **34**, 4513 (2001).
54. P. G. de Gennes, *J. Chem. Phys.*, **55**, 572 (1971).
55. M. Doi, *J. Polym. Sci., Part C: Polym. Lett.*, **19**, 265 (1981).
56. P. T. Callaghan and E. T. Samulski, *Macromolecules*, **33**, 3795 (2000).
57. H. Watanabe and T. Inoue, *Mater. Sci. Eng., A*, **442**, 361 (2006).
58. D. A. Vega, L. R. Gomez, L. E. Roth, J. A. Ressia, M. A. Villar, and E. M. Valles, *Phys. Rev. Lett.*, **95** (2005).
59. "Sounds and Vibration Damping with Polymers," R. D. Corsaro and L. H. Sperling, Ed., American Chemical Society, Washington, DC, 1990.
60. J. A. Grates, D. A. Thomas, E. C. Hickey, and L. H. Sperling, *J. Appl. Polym. Sci.*, **19**, 1731 (1975).
61. S. Yao, in "Advances in Interpenetrating Polymer Networks," vol. IV, D. Klempner and K. C. Frisch, Ed., Technomic, Lancaster, PA, 1994, p. 243.
62. H. Q. Xie, C. X. Zhang, and J. S. Guo, in "Interpenetrating Polymer Networks," D. Klempner, L. H. Sperling, and L. A. Utracki, Ed., American Chemical Society, Washington, DC, 1994, p. 557.
63. H. H. Winter and M. Mours, *Adv. Polym. Sci.*, **134**, 165 (1997).
64. K. Urayama, T. Miki, T. Takigawa, and S. Kobjiya, *Chem. Mater.*, **16**, 173 (2004).
65. H. P. Patil and R. C. Hedden, *J. Polym. Sci., Part B: Polym. Phys.*, **45**, 3267 (2007).

Kenji Urayama is currently an Associate Professor of Materials Chemistry at Kyoto University. He was born in Gifu Prefecture, Japan in 1967. He earned a B. Eng. degree in 1990 and M. Eng. degree in 1992 from Kyoto University under the supervision of Prof. Toshiro Masuda. He quitted the Ph.D. course and joined Prof. Shinzo Kohjiya's group as an Assistant Professor in Institute for Chemical Research at Kyoto University in 1994. Urayama received a D. Eng. degree in 1996 from Kyoto University. In 2003 he moved to the Department of Materials Chemistry at Kyoto University as a Lecturer, and was promoted to Associate Professor in 2005. His main interest focuses on the stimuli-response relationships of polymer networks, gels, and liquid crystal elastomers. His honors include Young Researcher Award of Society of Rheology, Japan (2005), Promising Researcher Award from Society of Material Science, Japan (2006), John H. Dillon Medal from Division of Polymer Physics in American Physical Society (2006), and Wiley Award from Society of Polymer Science, Japan (2007).

